Yttrium and Neodymium Di- and Monohalide Complexes Based on Scorpionate (Poly(pyrazolyl)borate) Ligands

David P. Long, A. Chandrasekaran, Roberta O. Day, and Patricia A. Bianconi*

Department of Chemistry, The University of Massachusetts at Amherst, Amherst, Massachusetts 01003

Arnold L. Rheingold

Department of Chemistry and Biochemistry, The University of Delaware, Newark, Delaware 19716

Received October 6, 1999

The syntheses of a series of well-characterized complexes of the type $Tp^RYX_2(solvent)_n$ (**1** and **2**, R = H, X = Br, Cl, solvent = THF, n = 2; **4**, R = Me, X = Cl, solvent = THF, n = 1; **5**, R = Me, X = Cl, solvent = 3,5-dimethylpyrazole, n = 1; **7**, R = Ph, X = Cl, solvent = THF, n = 1) and the novel solvent-free bis(poly-(pyrazolylborate) complexes $[(Tp^R)(Bp^{R'})YX]$ (**8**, R = R′ =Me, X = Cl; **9**, R = H, R′ = Ph, X = Br) are presented. The data demonstrate that the steric, dynamic, and coordination behavior of these complexes are heavily influenced by the choice of scorpionate ligand substituents, showing the versatility of this ligand system for catalyst design. The coordinated THF solvent molecules of complexes **1**, **2**, and **4** are seen to undergo a dynamic solvation/desolvation equilibrium in solution that is fast on the NMR time scale. The position of this equilibrium is solvent-dependent and can be evaluated in complex **4** by observation of the line broadening of the 3-methyl resonance in the ^1H NMR spectra taken in different deuterated solvents. Complex **5**, formed by slow hydrolysis of **4**, has been characterized by an X-ray diffraction structure determination and shown to adopt a distorted octahedral geometry that is thought to be similar to that of complex **4**. The Nd analogues of these complexes (**3**, R = H, X = I, solvent = THF, n = 2; **6**, R = Me, X = I, solvent = THF, n = 1) have been characterized by X-ray diffraction structure determinations: **3** shows a distorted capped octahedral structure, and **6** a distorted octahedral structure similar to that of **5**. The solvent-free complex **8** is shown by ^1H and ^{13}C NMR spectroscopic analysis to be nonfluxional in solution on the NMR time scale, although **9** appears able to weakly coordinate solvents containing donor groups such as halides.

Introduction

Scorpionate, or poly(pyrazolyl)borate, ligands, which include the tris-chelating hydrotris(pyrazolyl)borates (Tp) and the bis-chelating dihydrobis(pyrazolyl)borates (Bp), are attractive ancillary species for the stabilization of lanthanide complexes. Since their first synthesis by S. Trofimenko,[1] these ligands have found broad applications in coordination chemistry with nearly every metal of the periodic table.[2] Tp ligands display several characteristics similar to those of cyclopentadienyl systems;[3] however, their unique properties provide advantages that make them especially attractive for the synthesis of lanthanide complexes.[4]

The most useful feature of these ligands is their versatility in creating different steric environments around a metal by utilizing a modest degree of substitution. The addition of even small groups in the 3-positions of the pyrazolyl rings substantially changes the steric environment of the resulting complex, since these groups lie on three sides and in close proximity to the coordinating metal. Substituents in the 3-positions can also be used to control the stereochemical[5a,b] and electronic properties[6] of the ligands, thus permitting the design of very individual or chiral environments for specific metals or functions.

The first examples of hydrotris(pyrazolyl)borate lanthanide derivatives were homoleptic compounds of the type Tp_3Ln (Ln = Sc, Y, La, Ce−Lu).[7a,b] A large number of heteroleptic Tp lanthanide complexes have since been reported, most of which are eight-coordinate, of the type $Tp_2Ln(L)$ (L = bidentate ligand)[8a,b] or $(Tp^H)_2LnX(solv)$ (X = halide, solv = neutral coordinating solvent).[9] Lanthanide dihalidehydrotris(pyrazolyl)-borate complexes, Tp^RLnX_2 (Ln = any lanthanide, X = halide) have been little studied as precursors to derivatives of these metals,[10,11] though complexes of the types $Tp^{Me}YbCl_2(THF)$[10a] and $Tp^HLnCl_2(THF)_{1.5}$ (Ln = Er, or Y)[11] have been reported. For the complex $Tp^{Me}SmCl_2(L)$ (L = coordinating molecule), attempts at derivatization using such groups as Cp^-, OR^-,

(1) Trofimenko, S. *J. Am. Chem. Soc*. **1966**, *88*, 1842.
(2) Trofimenko, S. *Scorpionates: The Coordination Chemistry of Polypyrazolyborate Ligands*; Imperial College Press: London, 1999 and included references.
(3) Trofimenko, S. *Chem. Rev*. **1993**, *93*, 943.
(4) Santos, I.; Marques, N. *New J. Chem*. **1995**, *19*, 551 and included references.
(5) (a) Trofimenko, S.; LeCloux, D. D.; Tolman, W. B. *J. Am. Chem. Soc*. **1993**, *115*, 1153. (b) Keyes, M. C.; Young, V. G.; Tolman W. B. *Organometallics* **1996**, *15*, 4133.
(6) Dias, H. V. R.; Wang, Z.; Jin, W. *Inorg. Chem.* **1997**, *36*, 6205.
(7) (a) Bagnall, K. W.; Tempest, A. C.; Takats, J.; Masino, A. P. *Inorg. Nucl. Chem. Lett*. **1976**, *12*, 555. (b) Stainer, M. V. R.; Takats, J. *Inorg. Chem.* **1982**, *21*, 4050.
(8) (a) Moss, M. A.; Jones, C. J.; Edwards, A. J. *Polyhedron* **1988**, *7*, 79. (b) Moss, M. A.; Jones, C. J.; Edwards, A. J. *J. Chem. Soc., Dalton Trans*. **1989**, 1393.
(9) Reger, D. L.; Lindeman, J. A.; Lebioda, l. *Inorg. Chim. Acta* **1987**, *139*, 71.

10.1021/ic991179l CCC: $19.00
Published on Web 09/14/2000

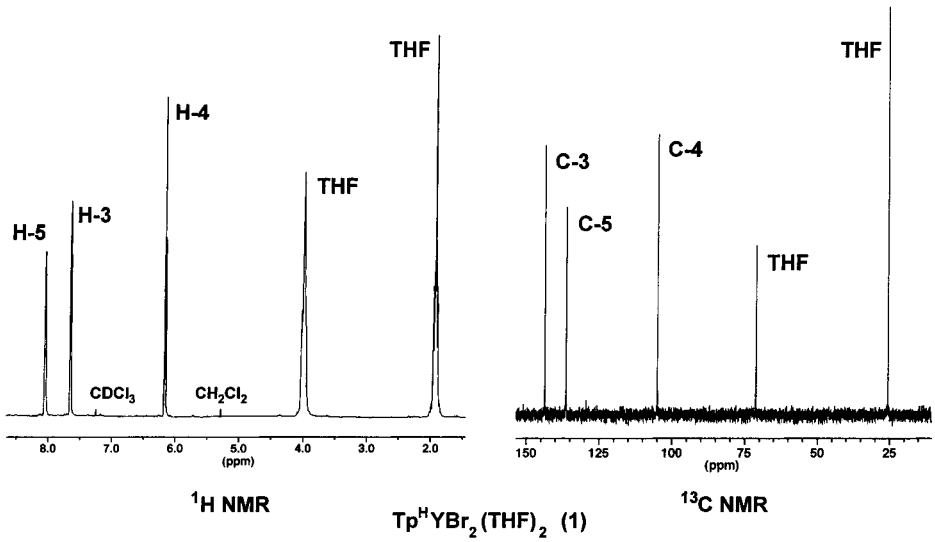

Figure 1. ^{1}H and ^{13}C NMR spectra of $[Tp^HYBr_2(THF)_2]$ (**1**) in $CDCl_3$. In the ^{13}C spectrum the $CDCl_3$ peak has been omitted for clarity.

Et_2N^-, or R^- failed due to ligand redistribution.[12] However, the Yb(II) complex $(Tp^{t-Bu,Me})YbI(THF)$ was found to be a precursor to several stable derivatives $(Tp^{t-Bu,Me})YbER$ [ER = $HBEt_3$, $N(SiMe_3)_2$, CCPh, CH_2SiMe_3, $CH(SiMe_3)_2$, H].[13]

This work presents syntheses and characterization of yttrium dihalide complexes incorporating variations of the Tp ligand, the alkyl and aryl derivatives of which we have previously reported to be catalysts for the polymerization of ethylene.[14] In addition, reactions between these THF-adduct Tp yttrium dihalide complexes and additional bis-chelating scorpionate ligands, Bp^R, to give unsolvated bispoly(pyrazolyl)borohydride yttrium monohalide complexes, $[(Tp^R)(Bp^{R'})Y-X]$, are reported.

Results and Discussion

Synthesis and Characterization of Hydrotris(pyrazolyl)-borate Yttrium(III) Dihalide Bistetrahydrofuranate $[Tp^HYX_2(THF)_2]$ (X = Br, Cl). Hydrotris(pyrazolyl)borate yttrium(III) dibromide bistetrahydrofuranate, $Tp^HYBr_2(THF)_2$ (**1**), and hydrotris(pyrazolyl)borate yttrium(III) dichloride bistetrahydrofuranate, $Tp^HYCl_2(THF)_2$ (**2**), were synthesized according to Scheme 1. The reactions were carried out at room temperature, since higher temperatures were found to encourage redistribution of ligands. Slow addition of the ligand to the reaction solution was performed to minimize possible formation of $(Tp^H)_2YX(THF)$, since this less hindered ligand can readily form bis-Tp complexes with large metals.[3,4] During the addition, the displacement reaction took place nearly as fast as the ligand dissolved and could be followed visually by the precipitation of the insoluble sodium halide salt. ^{1}H and ^{13}C NMR spectra of $Tp^HYBr_2(THF)_2$ (the NMR spectra of **2** are nearly identical to those of **1**) shows that the complex contains three equivalent pyrazoles (Figure 1), which indicates fluxional behavior that is fast on the NMR time scale (Table 1). Integration of the ^{1}H NMR spectra and elemental analyses indicate that two molecules of THF are coordinated to the yttrium of **1** and **2**, which cannot be removed by heating or vacuum.

Scheme 1

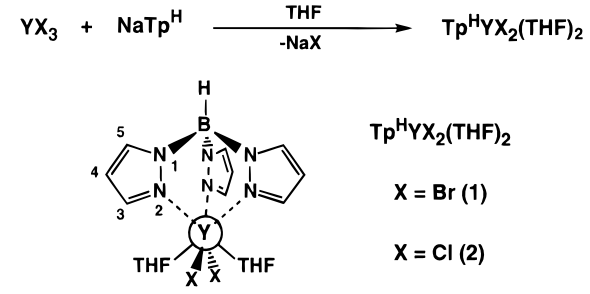

The crystallographic structures of $Tp^HYBr_2(THF)_2$ and $Tp^HYCl_2(THF)_2$ have not yet been determined, but the structures of these complexes are believed to resemble that of the neodymium diiodide analogue of these species, the synthesis and analysis of which has been previously described.[15] $Tp^HNdI_2(THF)_2$ (**3**) was found to adopt a seven-coordinate structure consisting of a tridentate Tp^H ligand, two bound iodide anions, and two coordinated THF molecules arranged in a distorted capped octahedron in which the seventh group has added to a triangular face of the complex (Figure 2). In the solid state **3** shows a mirror plane, which should generate inequivalent pyrazolyl rings in a 2:1 ratio, but again, this complex proved to have three equivalent rings in its NMR spectra, confirming a fast dynamic process in solution. Because of the structural similarity commonly displayed by analogous complexes of different lanthanide metals, and the similar fluxionality of these three complexes, $Tp^HYBr_2(THF)_2$ and $Tp^HYCl_2(THF)_2$ are expected to adopt solid state geometries similar to that of $Tp^HNdI_2(THF)_2$.

Synthesis and Characterization of Hydrotris(3,5-dimethylpyrazolyl)borate Yttrium(III) Dichloride Tetrahydrofuranate $[Tp^{Me}YCl_2(THF)]$ (4). The synthesis of hydrotris(3,5-dimethylpyrazolyl)borate yttrium(III) dichloride tetrahydrofuranate $Tp^{Me}YCl_2(THF)$ (**4**), incorporating the more sterically demanding Tp^{Me} ligand, does not require the synthetic precautions the smaller Tp analogue demands. Slow addition of KTp^{Me} is not

(10) (a) Apostolidis, C.; Carvalho, A.; Domingos, A.;, Kanellakopoulos, B.; Maier, R.; Marques, N.; Pires de Matos, A.; Rebizant, J. *Polyhedron* **1999**, *18*, 263. (b) Apostolidis, C.; Kanellakopoulos, B.; Maier, R.; Meyer, D.; Marques, N.; Rebizant, J. *21e Journees des Actinides*, Montechoro, Portugal, 1991.

(11) Masino, A. P. Ph.D. Thesis, University of Alberta, 1978.

(12) Carretas, J. M.; Marques, N. *First International Conference on f-Elements*, Leuven, 1990.

(13) (a) Hasinoff, L.; Takats, J.; Zhang, X. W.; Bond, A. H.; Rogers, R. D. *J. Am. Chem. Soc.* **1994**, *116*, 8833. (b) Maunder, G. H.; Sella, A.; Tocher, D. A. *J. Chem. Soc., Chem. Commun.* **1994**, 2689, (c) Ferrence, G. M.; McDonald, R.; Takats, J. *Angew. Chem., Int. Ed.* **1999**, *38*, 2233.

(14) Long, D. P.; Bianconi, P. A. *J. Am. Chem. Soc.* **1996**, *118*, 12453.

(15) Mercando, P. Ph.D. Thesis, The Pennsylvania State University, 1992.

Table 1. ^{1}H and ^{13}C NMR Data for Selected Tp^R Yttrium Halide Complexes

chemical shift[a]/coupling[b]	assignment
$Tp^HYBr_2(THF)_2$ (**1**)	
^{1}H (200 MHz, $CDCl_3$)	
1.92 (m)	THF
3.99 (m)	THF
6.16 (t) 3 H (J_{H-H} = 2.16)	H-4
7.65 (d) 3 H (J_{H-H} = 1.80)	H-3
8.05 (d) 3 H (J_{H-H} = 1.80)	H-5
^{13}C (75 MHz, $CDCl_3$)	
25.7 (s)	THF
71.1 (s)	THF
105.0 (s)	C-4
136.4 (s)	C-3
143.7 (s)	C-5
$Tp^MeYCl_2(THF)$ (**4**)	
^{1}H (200 MHz, C_6D_6)	
1.16 (m) 4 H	THF
2.09 (s) 9 H	5-Me
2.57 (br s)	3-Me
3.74 (m) 4H	THF
5.42 (s) 3H	H-4
^{13}C (75 MHz, d_8-THF)	
12.86 (s)	5-Me
14.14 (s)	3-Me
106.5 (s)	C-4
146.2 (s)	C-3
151.3 (s)	C-5
$(Tp^{Me})(Bp^{Me})YCl$ (**8**)	
^{1}H (200 MHz, $CDCl_3$)	
0.534 (s) 3 H	Tp^{Me} 3-Me
1.39 (s) 6 H	Bp^{Me} 3-Me
2.38 (2 peaks) 9 H	Tp^{Me} 5-Me, Tp^{Me} 3-Me
2.43, 2.44 (2 peaks) 12 H	Tp^{Me} 5-Me, Bp^{Me} 5-Me
5.52 (s) 1 H	Tp^{Me} H-4
5.67 (s) 2 H	Tp^{Me} H-4
5.77 (s) 2 H	Bp^{Me} H-4
^{13}C (75 MHz, $CDCl_3$)[c]	
9.66 (s)	Tp^{Me} 3-Me
11.67 (s)	Bp^{Me} 3-Me
11.92 (s)	Tp^{Me} 3-Me
13.02 (s)	Bp^{Me} 5-Me
13.17 (s)	Tp^{Me} 5-Me
14.39 (s)	Tp^{Me} 5-Me
105.63 (s)	Bp^{Me} C-4
105.78 (s)	Tp^{Me} C-4
144.32, 145.02, 145.15 (s)	Tp^{Me} C-3, Bp^{Me} C-3
149.40, 150.69, 150.77 (s)	Tp^{Me} C-5, Bp^{Me} C-5
$(Tp^H)(Bp^{Ph})YBr$ (**9**)	
^{1}H (200 MHz, $CDCl_3$)	
6.07 (t) 3 H (J_{H-H} = 2.18)	Tp^H H-4
6.45 (d) 2 H (J_{H-H} = 2.18)	Bp^{Ph} H-4
7.14 (br m) 6 H	meta and para Ph-H
7.40 (br m) 4 H	ortho Ph-H
7.50 (br d) 3 H	Tp^H H-3
7.57 (d) 2 H (J_{H-H} = 2.18)	Bp^{Ph} H-5
7.68 (d) 3 H (J_{H-H} = 1.70)	Tp^H H-5
^{13}C (75 MHz, $CDCl_3$)	
104.6 (s)	Bp^{Ph} C-4
104.9 (s)	Tp^H C-4
127.3 (s), 128.5 (s)	ortho and meta Ph-C
128.5 (s)	para Ph-C
132.4 (s)	Bp^{Ph} C-5
136.7 (s)	Tp^H C-5
137.2 (s)	ipso Ph-C
144.5 (s)	Tp^H C-3
154.6 (2 peaks)	Bp^{Ph} C-3

[a] Chemical shifts (in δ, ppm) are referenced to residual nuclei in $CDCl_3$ at 7.27 (^{1}H) or 77.0 (^{13}C), in C_6D_6 at 7.15 (^{1}H), and in d_8-THF at 23.5 (^{13}C). B−H resonances (3.5−6 ppm) are not marked. [b] First-order coupling constants (J) are reported in hertz. [c] All ^{13}C NMR were run proton decoupled. Measured proton intensities match those of expected values.

required in order to obtain **4** as the only product. Tp^MeYCl_2(THF) (**4**) was synthesized according to reaction 1. Elemental

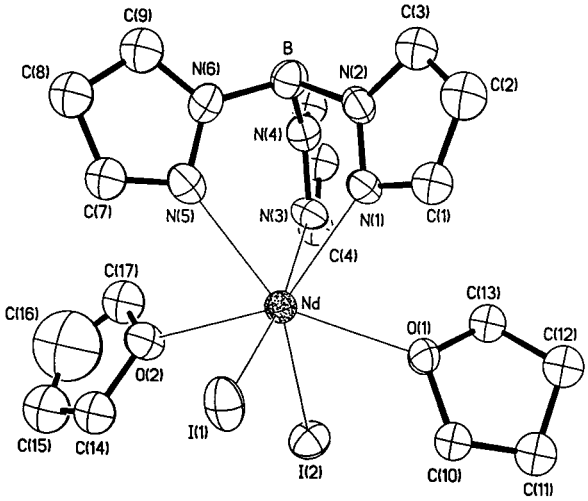

Figure 2. ORTEP plot of $Tp^HNdI_2(THF)_2$ (**3**) with thermal ellipsoids at the 30% probability level. Hydrogen atoms are omitted for clarity.

$$YCl_3 + KTp^{Me} \xrightarrow[-KCl]{THF} Tp^{Me}YCl_2(THF) \qquad (1)$$

anaylsis and ^{1}H NMR spectrum integration show one molecule of THF coordinated to the yttrium center of **4**, which again cannot be removed by heat, vacuum, or Soxhlet extraction.

Figure 3 shows the ^{1}H and ^{13}C NMR spectra of Tp^MeYCl_2(THF) taken in $CDCl_3$, at 30 °C. The ^{1}H spectrum shows three sharp resonances corresponding to the 3-Me, 5-Me, and H-4 protons of the pyrazoles in the expected ratio of 9:9:3. The resonances from the equivalent pyrazoles confirm that a dynamic process, possibly similar to that which occurs in $Tp^HYBr_2(THF)_2$ (**1**) and $Tp^HYCl_2(THF)_2$ (**2**), is also taking place in this complex, which is consistent with findings from past reports of $Tp^MeSmCl_2(THF)$.[12] The ^{13}C NMR spectrum shows the five expected resonances for the equivalent carbon atoms of the pyrazolyl rings, again confirming the complexes' fluxionality in solution. Interestingly, no coupling between nuclei of the ligand, ^{1}H or ^{13}C, and the yttrium metal ($I = {}^1/_2$) is observed, as is the case when the thallium ($I = {}^1/_2$) derivative of this ligand is synthesized.[16]

Unsolvated Tp lanthanide complexes have been shown to be sufficiently rigid in solution that their structures approximate those found in the solid state.[17] This suggests that the dynamic process equilibrating the pyrazolyl rings of **4** may be the dissociation and association of the coordinated solvent rather than the Tp ligand undergoing some form of fluxionality itself. Watson and Herskovitz and Marks and co-workers have extensively studied the bond strength and lability of coordinated solvents on lanthanide metallocenes[18] and have found that, for all solvents studied, solvation always lies far to the left, demonstrating the natural tendency of these metals to saturate themselves both sterically and electronically. Fast dissociation was observed down to low temperatures, with static structures not being reached until −65 °C for some THF-solvated lanthanide metallocenes. The dissociation rates changed depending on the solvent in which the complexes were dissolved: ligand dissociation processes were shown to be 2−3 times faster in cyclohexane than in toluene.

(16) Long, D. P. Ph.D. Thesis, The University of Massachusetts at Amherst, 1998.
(17) Stainer, M. V. R.; Takats, J. *J. Am. Chem. Soc.* **1983**, *105*, 410.
(18) (a) Watson, P. L.; Herskovitz, T. *ACS Symp. Ser.* **1983**, *212*, 459. (b) Nolan, S. P.; Stern, D.; Marks, T. J. *J. Am. Chem. Soc.* **1989**, *111*, 7844.

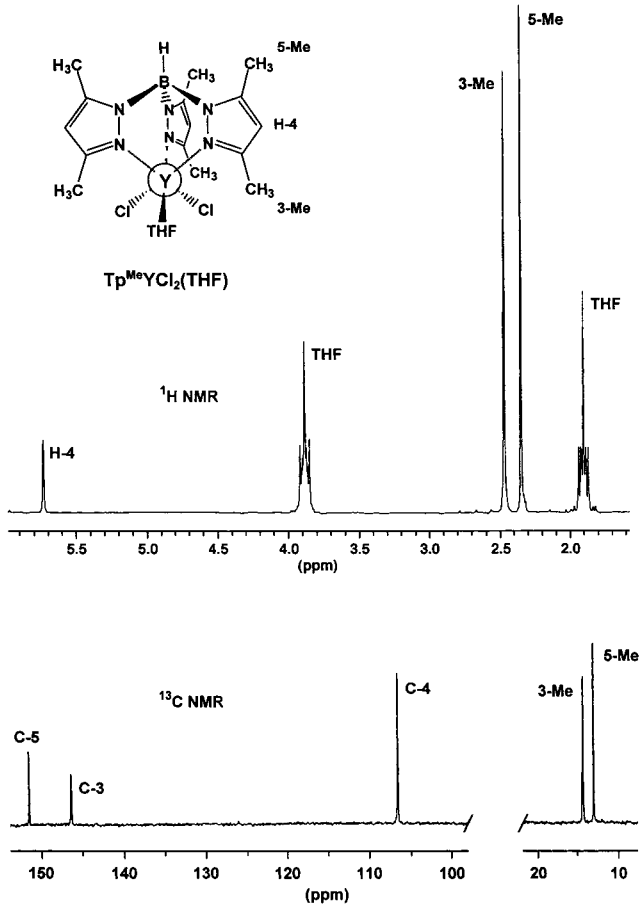

Figure 3. ^{1}H and ^{13}C NMR spectra of [$Tp^{Me}YCl_2$(THF)] (**4**) in d_8-THF. In the ^{13}C spectrum solvent peaks (d_8-THF) between 20 and 100 ppm have been omitted.

When a smiliar THF solvation/desolvation dynamic process was suspected in the yttrium complex $Tp^{Me}YCl_2$(THF) (**4**), attempts were made to quantify the dissociation of the solvent. Variable-temperature ^{1}H NMR spectroscopy was performed on $Tp^{Me}YCl_2$(THF) (**4**) in an attempt to measure the lability of the coordinated THF by conducting a coalescence experiment. The ^{1}H NMR spectrum of $Tp^{Me}YCl_2$(THF) with 1 equiv of THF added was acquired on a 200 MHz Bruker NMR in $CDCl_3$ and in d_8-toluene from 50 to −70 °C with spectra collected every 20 °C. Although the peaks assigned to the THF protons of the complex were observed to broaden significantly as the temperature decreased, the limiting temperature could not be reached. Since the low-temperature limit was not reached by −70 °C, it can be concluded that the dissociation of the THF is still a dynamic process at this temperature. Had the complex reached its static structure where the THF is "frozen" into place on the yttrium, the 3-Me and pyrazole H-4 peaks should have been observed to split into two separate resonances in a 2:1 ratio indicative of C_s symmetry.[12] That the static structure for $Tp^{Me}YCl_2$(THF) (**4**) could not be observed by −70 °C may suggest that the larger steric bulk of the Tp^{Me} ligand permits (or forces through steric interactions) a faster dissociation of the coordinated THF compared to the analogous THF-solvated lanthanide metallocenes. In support of this, broadening of the 3-methyl proton resonances of **4** relative to the 5-methyl groups and to the methyl resonances of the free ligand is seen in all solvents (except THF, see below). NOE experiments (500 MHz Bruker NMR, 25 °C in d_6-benzene) showed steric interactions between the 3-methyl protons and the bound THF, which suggests restricted rotation of the methyl groups: a −2% NOE on the THF's β-protons was observed when the 3-methyl protons were irradiated.

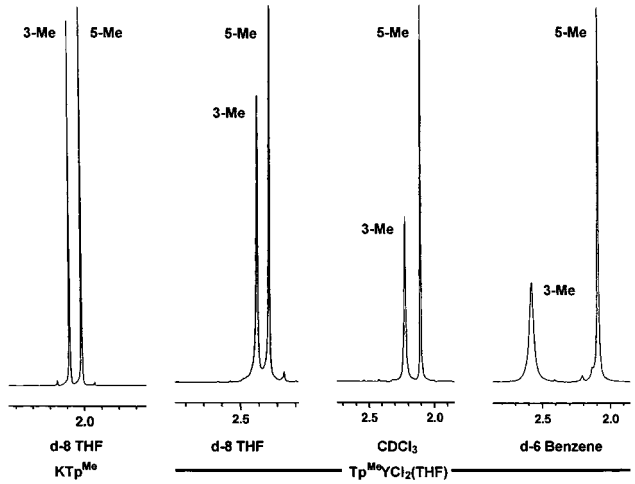

Figure 4. 3,5-Dimethyl region in the ^{1}H NMR spectra of KTp^{Me} and $Tp^{Me}YCl_2$(THF) (**4**), acquired in various deuterated solvents. THF resonances are omitted for clarity.

That broadening at successively lower temperatures was seen in the VT NMR spectroscopy experiments in the THF resonances indicates that this group is the one involved in the fluxionality observed in **4**. This is supported by the ^{1}H spectrum of **4** observed when the THF is replaced by a bulkier ligand. Carretas and Marques reported in their investigations of $Tp^{Me}SmCl_2$(THF) that replacement of the coordinated THF with a larger molecule stopped the observed dynamic process of solvation/desolvation by increasing the reaction's energy barrier for solvent dissociation.[12] Similarly, in **4**, the dynamic process of solvation/desolvation is stopped when a larger coordinating solvent is used. When the synthesis of **4** is carried out in 3,5-dimethyl THF, ^{1}H NMR spectroscopy shows a static structure, with the larger 3,5-dimethyl THF coordinated, and the Tp^{Me} ligand showing inequivalent pyrazoles in the expected 2:1 ratio.

Another method used to probe the fluxionality of **4** was the use of different solvents for ^{1}H NMR spectroscopy. Solvent association/dissociation dynamic processes have a large rate dependence on the bulk solvent, and this dependence was observed by Watson and Herskovitz.[18] In the case of $Tp^{Me}YCl_2$(THF) (**4**), because THF dissociation is fast down to −70 °C, we could not directly measure the difference in rates in various solvents, but their effect could easily be observed due to the structure of the Tp^{Me} ligand. The amount of exchange and/or T_2 broadening of the 3-methyl resonances is greatly affected by the residence time of the THF on the metal, and therefore by the differing rates of THF dissociation in various bulk solvents.

^{1}H NMR spectroscopic analysis performed on $Tp^{Me}YCl_2$(THF) (**4**) in various deuterated solvents at 25 °C shows that the environment experienced by the 3-methyl substituents can be dramatically altered by the choice of solvent used to dissolve the complex (Figure 4). The deuterated solvents $CDCl_3$, d_8-THF, d_5-chlorobenzene, d_6-benzene, and d_8-toluene were used, and a large difference in the broadening of the 3-methyl resonances, depending on the solvent chosen, was found. The resonances of the ligand's 5-methyl substituents did not change with solvent because the 5-methyl groups of the Tp^{Me} ligand point away from the metal's coordination sphere, giving these methyl groups the greatest amount of rotational freedom, longest T_2 relaxation times, and sharpest NMR resonances. In fact, the

resonances of the 5-methyl substituents can be used as a visual reference for how sterically crowded the 3-methyl protons have become (due to longer residence time on the yttrium of the THF) simply by comparing their relative heights, since in the KTp^{Me} ligand, where neither substituent is experiencing a great deal of steric interaction or ligated solvent exchange, their heights are nearly identical (Figure 4). From the increasing broadening of the 3-methyl resonances, it was found that solvents increase the steric rigidity of the complex $Tp^{Me}YCl_2(THF)$ in the order d_8-THF < $CDCl_3$ < d_5-chlorobenzene < d_6-benzene ≈ d_8-toluene (Figure 4).

In these spectra, increasing steric rigidity of the complex (as evidenced by increased exchange and/or T_2 broadening of the 3-methyl proton resonances) is attributed to increased retention time of the bound THF ligand in the different bulk solvents. However, in the case of d_8-THF, rapid exchange with the solvent, rather than a single THF association/dissociation, apparently occurs, so that no one THF molecule has a long enough residence time on the yttrium to dephase the nearby 3-methyl protons or to cause the appearance of the static structure. No significant exchange or T_2 broadening is seen, and the resonance of the 3-methyl protons becomes nearly identical in appearance to that of the 5-methyl protons and that of the free ligand.

The varying ^{1}H NMR resonances of the 3-methyl groups in $Tp^{Me}YCl_2(THF)$, caused by the different levels of steric rigidity that varying retention times of ligated THF produce, offer an unusual method by which the environment around the metal of this catalyst precursor may be visually assessed. It may be possible to use this information to choose the proper-sized lanthanide metal, alkylating agent, Tp substituent, and solvent for particular olefin polymerizations, all based on how changes in these variables affect the coordination sphere around the metal. Similar, more pronounced, variations in the broadening of the ^{1}H NMR resonances of the pyrazolyl 3-methyl groups and the yttrium alkyl substituents are observed in the dialkyl derivative of **4**, $Tp^{Me}Y(CH_2SiMe_3)_2(THF)$, which is an active polymerization catalyst,[14,19] thus demonstrating that it may be possible to use ^{1}H NMR spectroscopy as a probe of the coordination environment at precisely the region where all the steps of insertion polymerization and polymer growth take place.

Crystal Structure of $Tp^{Me}YCl_2$(3,5-dimethylpyrazole) (5). Attempts to obtain a molecular structure of the complex $Tp^{Me}YCl_2(THF)$ (**4**) by X-ray analysis failed due to the inability to grow suitable crystals. However, a hydrolysis product of **4** did form crystals, which were analyzed by X-ray diffraction. The hydrolysis was performed by slow exposure to ambient atmosphere at room temperature of an analytically pure sample of $Tp^{Me}YCl_2(THF)$ in methylene chloride. The slow hydrolysis of the complex yielded large colorless rectangular crystals, which were cut and sealed in capillary tubes for X-ray analysis. The hydrolysis product of **4** was thus determined to be the monomeric complex $Tp^{Me}YCl_2$(3,5-dimethylpyrazole) (**5**), which was obtained in crystalline form as the 1:0.5 methylene chloride solvate. The molecular geometry of the complex and the atom-labeling scheme are shown in the ORTEX plot of Figure 5, while selected bond lengths and angles are given in Table 2. Crystal and refinement data, atomic coordinates, thermal parameters, and a complete list of bond lengths and angles are provided as Supporting Information. The complex contains a six-coordinate yttrium metal with a tridentate Tp^{Me} ligand, two bound chloride ions, and a coordinated neutral molecule of 3,5-dimethylpyrazole arranged in a distorted octahedron.

(19) Long, D. P.; Bianconi, P. A. To be submitted for publication.

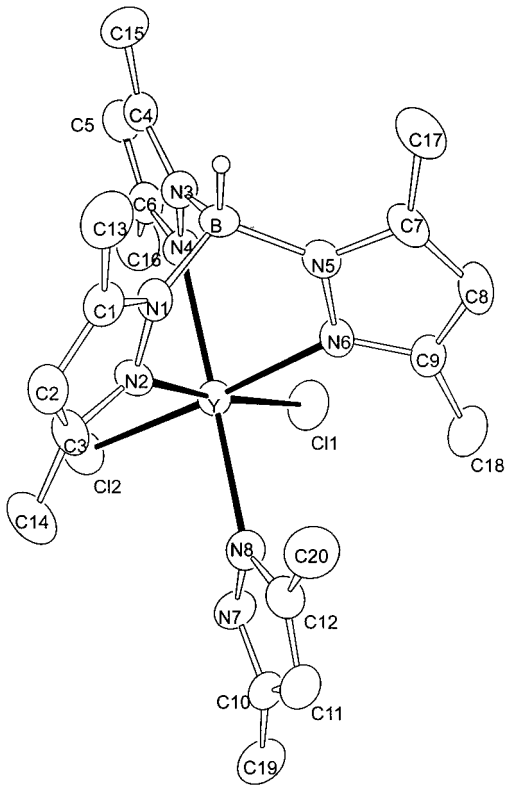

Figure 5. ORTEX plot of $Tp^{Me}YCl_2$(3,5-dimethylpyrazole) (**5**·0.5CH_2Cl_2) with thermal ellipsoids at the 40% probability level. Hydrogen atoms and atoms of the methylene chloride of solvation are omitted for clarity.

Table 2. Selected Bond Distances (Å) and Angles (deg) for $Tp^{Me}YCl_2$(3,5-dimethylpyrazole)·$^1/_2CH_2Cl_2$ (**5**·0.5CH_2Cl_2)[a]

Y−N(4)	2.368(6)	Y−N(8)	2.428(6)
Y−N(2)	2.418(5)	Y−Cl(2)	2.553(2)
Y−N(6)	2.420(5)	Y−Cl(1)	2.556(2)
N(4)−Y−N(2)	79.4(2)	N(6)−Y−Cl(2)	170.82(14)
N(4)−Y−N(6)	79.3(2)	N(8)−Y−Cl(2)	95.2(2)
N(2)−Y−N(6)	78.6(2)	N(4)−Y−Cl(1)	98.1(2)
N(4)−Y−N(8)	164.3(2)	N(2)−Y−Cl(1)	173.22(14)
N(2)−Y−N(8)	91.9(2)	N(6)−Y−Cl(1)	94.79(14)
N(6)−Y−N(8)	86.2(2)	N(8)−Y−Cl(1)	89.06(14)
N(4)−Y−Cl(2)	98.2(2)	Cl(2)−Y−Cl(1)	94.31(8)
N(2)−Y−Cl(2)	92.29(14)		

[a] Atoms are labeled to agree with Figure 5. Esd's in parentheses.

Hydrolysis occurring at the B−N bond of the Tp^{Me} ligand to form free pyrazole may reflect the high degree of steric saturation around the coordinated yttrium, kinetically slowing the hydrolysis of the chloride ligand. Similar reactivity (hydrolysis of Tp^{Me} to produce a coordinated pyrazole) is seen in the complexes $[LnCl(\mu\text{-}Cl)Tp^{Me}(3,5\text{-dimethylpyrazole})]_2$ (Ln = Pr, Nd, Yb), which are formed when stoichiometric amounts of the lanthanide trichlorides are refluxed or stirred in THF with the Tp^{Me} ligand.[10,11] Once free molecules of 3,5-dimethylpyrazole are present, displacement of the coordinated THF can occur, as has been reported for $Tp^H{}_2YCl(THF)$, in which free pyrazole has been shown to be able to replace the coordinated THF, forming $Tp^H{}_2YCl$(pyrazole).[20]

The solid state structure of $Tp^{Me}YCl_2(THF)$ (**4**) is presumed to be similar to that of $Tp^{Me}YCl_2$(3,5-dimethylpyrazole) (**5**), since the only difference between these complexes is the solvent

(20) Reger, D. L.; Lindeman, J. A.; Lebioda, L. *Inorg. Chem.* **1988**, *27*, 3923.

Table 3. Comparison of Bond Lengths and Angles for **5**·0.5CH_2Cl_2, $Tp^{Me}NdI_2(THF)$ (**6**), and $Tp^{Me}YbCl_2(Me\text{-}pz)\cdot THF$[11]

	$Tp^{Me}YCl_2(Me\text{-}pz)$	$Tp^{Me}NdI_2(THF)$	$Tp^{Me}YbCl_2(Me\text{-}pz)$
av Ln−N(Tp) bond length (Å)	2.402	2.494	2.368
Ln−(solvent) bond length (Å)	2.428	2.415	2.376
av Ln−X (halide) bond length (Å)	2.555	3.048	2.520
X−Ln−X bond angle (deg)	94.31	96.1	97.78
range of orthogonal bond angles (deg)	78.6−98.2	75.2−99.7	76.7−97.8

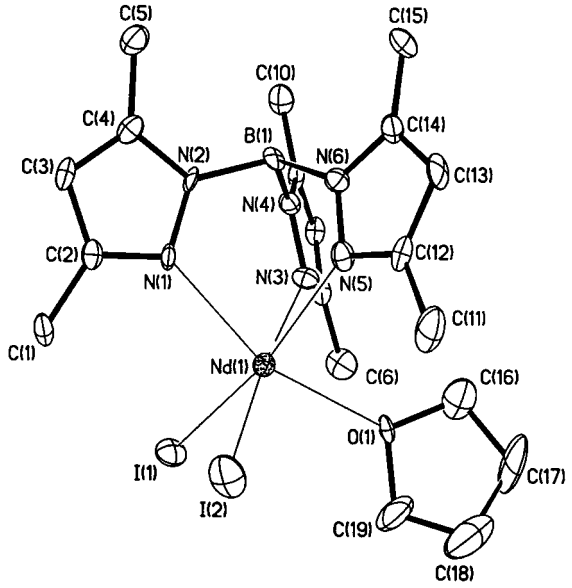

Figure 6. ORTEP plot of $Tp^{Me}NdI_2(THF)$ (**6**) with thermal ellipsoids at the 30% probability level. Hydrogen atoms are omitted for clarity.

coordinated in the vacant site of the yttrium. The molecular structures of the analogous neodymium diiodide complex $Tp^{Me}NdI_2(THF)$ (**6**)[15] (Figure 6) and the analogous Yb dichloride complexes[11] $Tp^{Me}YbCl_2(THF)$ and $Tp^{Me}YbCl_2$(3,5-dimethylpyrazole) have previously been determined. The Nd and Yb complexes also contain a six-coordinate lanthanide center surrounded by a tridentate Tp^{Me} ligand, two bound halide ions, and a coordinated molecule of THF or 3,5-dimethylpyrazole arranged in a distorted octahedron. The complex $Tp^{Me}NdI_2(THF)$ was shown to contain Nd−N bond lengths ranging from 2.461(13) to 2.521(15) Å, Nd−I bond lengths of 3.040(2)−3.055(2) Å, and a Nd−O bond length of 2.415(14) Å. The range of bond angles between orthogonals, a measure of distortion from true octahedral geometry, is 75.2(5)−99.7(4)°. The complexes $Tp^{Me}YbCl_2(solvent)$[11] were shown to contain Yb−N bond lengths ranging from 2.30(2) to 2.39(2) Å, Yb−Cl bond lengths of 2.495(7)−2.529(6) Å, Yb−O and Yb−N (Me_2pzH) bond lengths of 2.294(13) and 2.376(4) Å, respectively, and a range of bond angles between orthogonals of 79.5(5)−98.5(4)°. These data can be compared to the structure of $Tp^{Me}YCl_2$(3,5-dimethylpyrazole), where Y−N(Tp) bond lengths range from 2.368(6) to 2.428(6) Å and Y−Cl bond lengths are 2.553(2) and 2.556(2) Å, with the distortion from a true octahedron ranging from 78.6 (2)° to 98.2 (2)°. These data have been summarized in Table 3 and illustrate the contraction of bond lengths in $Tp^{Me}YCl_2$(3,5-dimethylpyrazole) relative to the Nd−THF analogue, and the bond length expansion relative to the Yb analogue, as well as **5**'s closer approximation to true octahedral geometry over **6**. These relative bond lengths and angles may arise from the complexes' varying size of the central metal ion.

Synthesis and Characterization of Hydrotris(3-phenylpyrazolyl)borate Yttrium(III) Dichloride Tetrahydrofuranate [$Tp^{Ph}YCl_2(THF)$] (7). Although phenyl rings are larger substituents than methyl groups, when placed in the 3-position of the Tp ligand the freely rotating phenyl rings can turn in any direction to minimize steric interactions for incoming coordinating species. Thus, the pocket defined by the three phenyl substituents can change shape depending on what other ligands are coordinated to the metal. Several papers have appeared in the literature describing the structures of metal complexes, mostly d-block metals, incorporating Tp^{Ph} ligands. It has been found that the twist angle between the phenyl rings and the plane defined by the pyrazolyl group can range anywhere from 2° to 62°. This large range of twisting was attributed to steric interactions between the Tp^{Ph} ligand's 3-phenyl groups and other coordinated ligands.[21a−c] That the phenyl substituents can twist in order to minimize steric interactions led us to synthesize dihalide complexes of this ligand to compare their stability and dynamic processes to those found in the analogous, theoretically less sterically congested, Tp^{H} andTp^{Me} complexes.

Hydrotris(3-phenylpyrazolyl)borate yttrium(III) dichloride tetrahydrofuranate, [$Tp^{Ph}YCl_2(THF)$] (**7**), was synthesized according to reaction 2.

$$YCl_3 + KTp^{Ph} \xrightarrow[-KCl]{THF} Tp^{Ph}YCl_2(THF) \qquad (2)$$

It was determined by ^1H NMR spectroscopy and elemental analysis that **7**, like the smaller Tp^{Me} complex, contains one coordinated THF molecule, giving the formula of $Tp^{Ph}YCl_2$(THF) (**7**). Extensive recrystallization is necessary in order to obtain pure material, possibly due to loss of coordinated THF. Figure 7 illustrates the change in the ^1H NMR spectrum between the ligand KTp^{Ph} and the yttrium complex $Tp^{Ph}YCl_2(THF)$ (**7**): coordination of the $YCl_2(THF)$ fragment into the Tp^{Ph} ligand disrupts the equivalency of the aromatic protons, possbily due to restricted rotation of the phenyl rings in the more sterically congested metal complex. Also, the 4H protons of the pyrzole rings exhibit several environments, suggesting fluxional behavior in **7** which is more complicated than that found in derivatives of the Tp and Tp^{Me} ligands. Whether this possible fluxionality involves a solvation/desolvation, varying coordination numbers for the pyrazolyl rings, or a combination of these and other processes has not been determined.

Synthesis and Characterization of [Hydrotris(3,5-dimethylpyrazolyl)borate][dihydrobis(3,5-dimethylpyrazolyl)-borate] Yttrium(III) Chloride, [(Tp^{Me})(Bp^{Me})YCl] (8). Since it has long been determined that molecules of coordinated solvent can severely interfere with the activity of early transition metal and lanthanide metallocene catalysts, syntheses of unsolvated scorpionate yttrium halide complexes were investigated.[13,22a,b]

The sterically crowded bispoly(pyrazolyl)borohydride lanthanide complex (Tp^{Me})(Bp^{Me})YCl (**8**) was prepared according to Scheme 2.

(21) (a) Rheingold, A. L.; Ostrander, R. L.; Haggerty, B. S.; Trofimenko, S. *Inorg. Chem.* **1994**, *33*, 3666. (b) Perkinson, J.; Brodie, S.; Yoon, K.; Mosny, K.; Carrol, P. J.; Morgan, T. V.; Burgmayer, S. N. *Inorg. Chem.* **1991**, *30*, 719. (c) Eichhorn, D. M.; Armstrong, W. H. *Inorg. Chem.* **1990**, *29*, 3607.

(22) (a) Takats, J.; Zhang, X. W.; Day, V. W.; Eberspacher, T. A. *Organometallics* **1993**, *12*, 4286. (b) Domingos, A.; Marques, N.; Matos, A.; Santos, I.; Silva, M. *Organometallics* **1994**, *13*, 654.

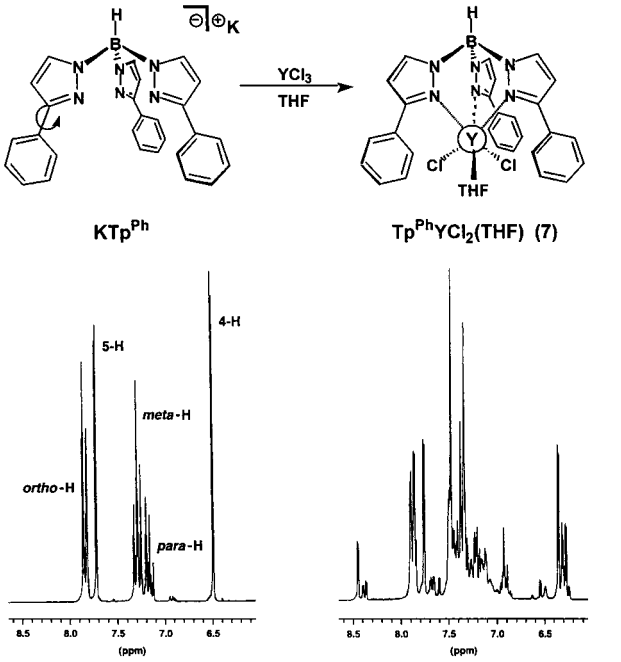

Figure 7. ^{1}H NMR spectra of KTp^{Ph} and $Tp^{Ph}YCl_2(THF)$ (**7**) in d_8-THF.

Scheme 2

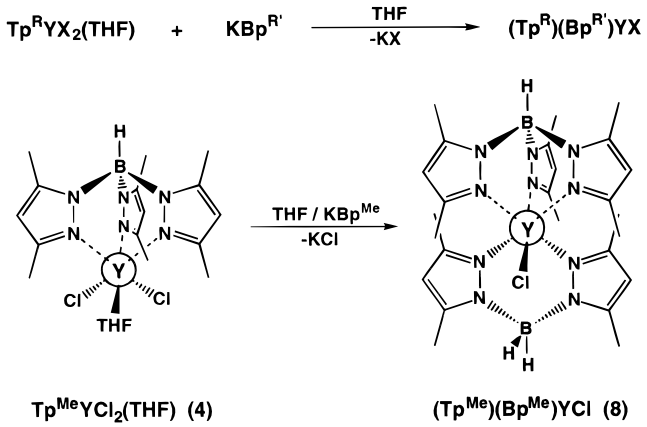

Characterization of this product by ^{1}H NMR and ^{13}C NMR spectroscopy and elemental analysis confirms the complex to be the unsolvated $(Tp^{Me})(Bp^{Me})YCl$, and, unlike the previously discussed complexes, **8** was found to adopt a static structure in solution. NMR spectroscopic analysis also suggests that the structure of the molecule is that of an octahedral complex containing a plane of symmetry relating the two pyrazolyl rings of the Bp^{Me} ligand and two of the pyrazolyl rings of the Tp^{Me} ligand. The ^{1}H NMR spectrum (Figure 8A) shows that **8** is completely free of coordinating solvents and contains inequivalent 3,5-dimethylpyrazolyl groups. The H-4 region (Figure 8B) is the most informative of the exact pyrazolyl ratio due to the simple resonance pattern observed for $(Tp^{Me})(Bp^{Me})YCl$. The ^{1}H NMR spectrum shows three peaks in the H-4 region corresponding to the H-4 protons from both the Tp^{Me} and the Bp^{Me} ligands. Two resonances for the Tp H-4 protons shows that the Tp^{Me} pyrazolyl groups are inequivalent, and are found in the ratio of 2:1 as expected for a static structure. Both Bp^{Me} pyrazolyl groups are equivalent and integrate correctly with the Tp^{Me} H-4 resonances to give a Tp:Bp ratio of 1:1. The Tp^{Me} H-4 proton observed at 5.52 ppm originates from the pyrazolyl group trans to the chloride anion, while the peak at 5.67 ppm

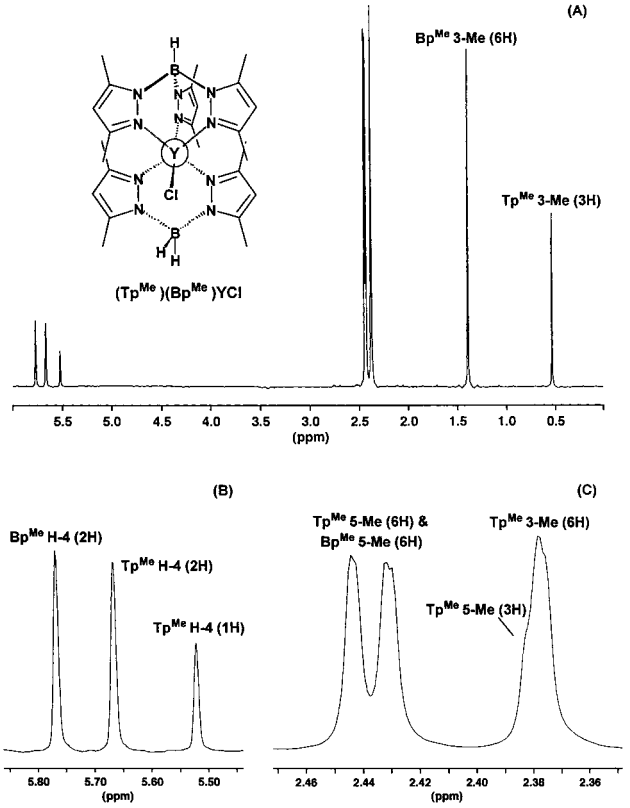

Figure 8. A. ^{1}H NMR spectrum of $(Tp^{Me})(Bp^{Me})YCl$ (**8**) in $CDCl_3$. B. Expanded view of the H-4 region of the ^{1}H NMR spectrum of **8**. C. Expanded view of the 3,5-dimethyl region around 2.5 ppm of the ^{1}H NMR spectrum of **8**.

is caused by the two Tp^{Me} H-4 protons on the pyrazolyl groups on either side of the mirror plane.

The 3,5-dimethyl region in the ^{1}H NMR spectrum of **8** is more complicated due to the overlapping of several peaks. The predicted structure for $(Tp^{Me})(Bp^{Me})YCl$ should give rise to six methyl resonances. Although one peak coincidentally overlaps with another set, each of these methyl signals is observed and can be identified in the ^{1}H NMR spectrum of **8** (Table 1). The peak integrating to a single methyl group observed at 0.535 ppm (2 ppm upfield from that of the 3-methyl protons of **4**) is assigned as the 3-Me group of the Tp^{Me} ligand that lies in the mirror plane of the complex. This observed shift to a higher field strength is attributed to the substituent lying between the two 3-Me groups of the Bp^{Me} ligand, effectively shielding this methyl group. The two equivalent 3-Me groups of the Bp^{Me} ligand responsible for this shielding are found at the next highest field strength at 1.39 ppm and integrate properly for two methyl groups. Between 2.3 and 2.5 ppm lie several resonances that integrate correctly for the remaining seven 3- and 5-methyl groups of both ligands (Figure 8c) and appear as three sets of peaks. Both the 3- and 5-methyl groups are in the proper ratio of 1:1, and the Tp^{Me} substituents are inequivalent and found in a 2:1 ratio as expected for the predicted structure containing a mirror plane.

Carbon NMR spectroscopy also supports the formation of $(Tp^{Me})(Bp^{Me})YCl$ in the octahedral geometry discussed above. Six methyl carbon resonances are predicted for the structure illustrated in Scheme 2 and are observed from 9.0 to 15.0 ppm (Figure 9). The C-3 and C-5 carbon atoms of the pyrazolyl rings of both ligands are also related by the mirror plane, resulting in three signals for each type of carbon.

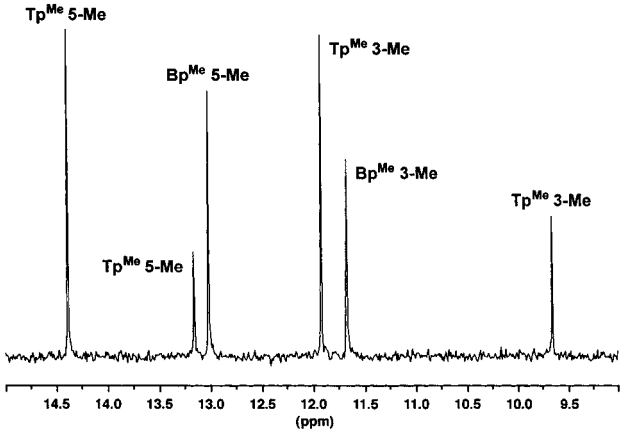

Figure 9. Expanded view of the methyl region of the ^{13}C NMR spectrum of **8** in $CDCl_3$.

These analyses by ^1H and ^{13}C NMR spectroscopy, as well as elemental analysis, confirm the addition of 1 equiv of Bp^{Me} ligand to $Tp^{Me}YCl_2(THF)$. The resulting complex **8** appears to assume octahedral geometry and so completely displaces the coordinated molecule of tetrahydrofuran, forming the unsolvated complex. The active yttrium chloride bond on $(Tp^{Me})(Bp^{Me})$-YCl should be capable of derivatization to alkyl or hydride species, and research into this possibility is currently underway.

Synthesis and Characterization of [Hydrotris(pyrazolyl)-borate][dihydrobis(3-phenylpyrazolyl)borate] Yttrium(III) Bromide, [$(Tp^H)(Bp^{Ph})$YBr] (9). Once the formation of an unsolvated monohalide yttrium complex was confirmed by the synthesis and characterization of **8**, it was decided to attempt this same reaction with yttrium dihalide complexes which incorporate the much less sterically crowded Tp^H ligand. Molecular modeling of $(Tp^R)(Bp^{R'})$YX complexes (constructed from crystal data of **5**) suggests that the 3-substituents on the Tp^R ligand will be the only groups on either scorpionate ligand that may hinder the approach and coordination of a monomer if derivatives of the complexes are used as polymerization catalysts. These 3-substitutents of the Tp^R ligand lie near the active bond (Y−R or Y−H, in **8** and **9** still Y−X), thus determining the steric crowding around the presumptive point of olefin insertion. The 3-substituents on the Bp^R ligand instead lie in the pockets of the Tp ligand adjacent to the "active" pocket and should not hinder the approach of a monomer to the active site. This is supported by the ^1H NMR spectrum of (Tp^{Me})-(Bp^{Me})YCl (**8**), in which it was observed that the Bp^{Me} 3-methyl groups greatly affected the lone 3-methyl group on the Tp^{Me} ligand trans to the chloride ion. In order for such an interaction to be occurring, the R groups of the Bp^{Me} ligand must reside as modeled in the inactive pockets of the Tp^{Me} ligand. In this position, the 3-substituents on the Bp^R ligand should act as stabilizing groups by protecting two of the three pockets around the metal generated by the Tp^H ligand and should help to increase the complexes' barrier to redistribution and their overall solubility. If so, bispoly(pyrazolyl)borohydride yttrium complexes of the type $(Tp^H)(Bp^R)$YR′ should offer the highest level of steric unsaturation at the Y−R′ bond of any combination of bis and tris scorpionate ligands, because the 3-substituents in Tp^H being protons create the most unhindered site for approaching olefins. The 3-substituents on the Bp^R ligand, however, should help to stabilize the complex by protecting the metal center on its two remaining sides while not interfering with any possible catalytic activity.

Synthesis of $(Tp^H)(Bp^{Ph})$YBr (**9**) was analogous to that of **8** (Scheme 3).

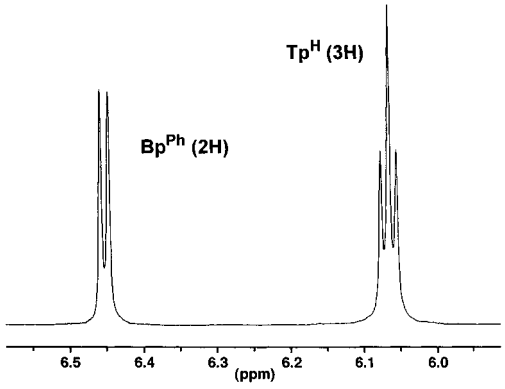

Figure 10. Expanded view of the H-4 region of the ^1H NMR spectrum of $(Tp^H)(Bp^{Ph})$YBr (**9**) in $CDCl_3$.

Scheme 3

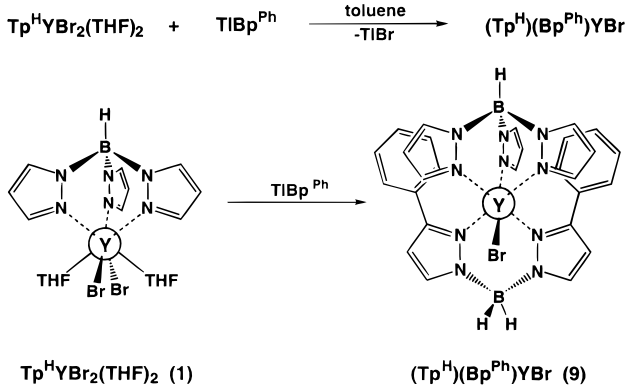

Characterization of **9** was again performed by proton and carbon NMR spectroscopy and elemental analysis. Elemental analysis confirms the proper ratios of C, H, N, and Br for the expected unsolvated monobromide yttrium complex, supporting the formula $(Tp^H)(Bp^{Ph})$YBr as the final product (extensive recrystallization is needed, however, to completely remove all traces of the fairly soluble TlBr). The ^1H NMR spectrum (Table 1) also confirms the product to be $(Tp^H)(Bp^{Ph})$YBr, although the expected spectral pattern, as described previously for (Tp^{Me})-(Bp^{Me})YCl (**8**), is not observed. ^1H NMR spectroscopy confirms that the ligands are in the proper ratio of 1:1 relative to each other, but the expected mirror plane of symmetry in the complex is not seen. The H-4 region (Figure 10) in the ^1H NMR spectrum of $(Tp^H)(Bp^{Ph})$YBr (**9**) shows two resonances. A triplet centered at 6.07 ppm corresponds to the H-4 protons of the Tp^H ligand, while a doublet at 6.45 ppm arises from the Bp^{Ph} ligand. These peaks integrate to each other in the ratio of 3:2, respectively. This suggests that the three H-4 protons of the Tp^H ligand are equivalent, as are the two H-4 protons of the Bp^{Ph} ligand. While the introduction of a mirror plane is expected to make equivalent the two H-4 protons of the Bp^{Ph} ligand, the Tp^H H-4 protons should be inequivalent in the same manner seen in (Tp^{Me})-(Bp^{Me})YCl (**8**): two Tp^H H-4 triplets in a ratio of 2:1 should be observed. Although the presence of the single doublet for the Bp^{Ph} H-4 protons suggests that a mirror plane does exist in the complex, the observation of the single triplet for the Tp^H H-4 protons does not, but may suggest instead that the complex is fluxional in solution, as discussed below.

The remaining proton resonances of $(Tp^H)(Bp^{Ph})$YBr (**9**) fall between 7.0 and 7.7 ppm (Figure 11). A large multiplet made up of sharp resonances is observed centered at 7.13 ppm, which integrates to six protons. These resonances are assigned to overlapping meta (4 H) and para (2 H) protons of the phenyl

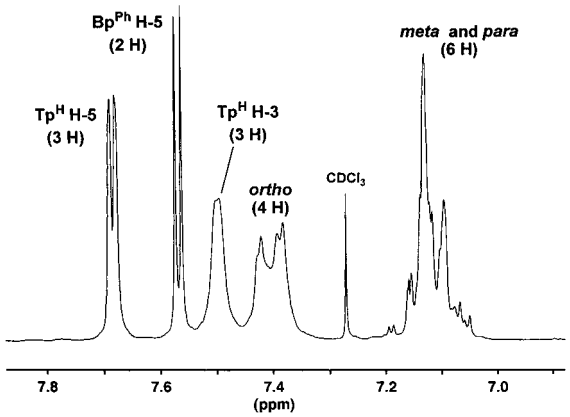

Figure 11. Expanded view of the aromatic region of the ^{1}H NMR spectrum of $(Tp^H)(Bp^{Ph})YBr$ (**9**) in $CDCl_3$.

groups on the Bp^{Ph} ligand, on the basis of their chemical shift and integration. Two doublets are observed at 7.68 ppm (3 H) and 7.57 ppm (2 H), which can be assigned from NMR spectroscopic analysis of other scorpionate ligands and complexes as being the H-5 protons from the Tp^H ligand and the Bp^{Ph} ligand, respectively.

The final resonances observed between 7.0 and 7.7 ppm appear as highly relaxed signals, unlike the sharp and distinct peaks just described. The broadening of these particular resonances supports the predicted octahedral geometry of **9**. Between 7.30 and 7.45 ppm a broad set of peaks integrating to four hydrogens is assigned to the ortho protons of the phenyl substituents. A broad peak at 7.50 ppm appears to be a doublet and integrates correctly for the H-3 protons of the Tp^H ligand. The high degree of line broadening observed in these sets of proton resonances is attributed to their restricted environment and close contacts in **9**, since these peaks usually appear distinct and sharp under normal conditions. Molecular modeling of the octahedral complex suggests close contact interactions for only the ortho protons and the H-3 protons of the Tp^H ligand as the phenyl substituents attempt to rotate. The observation of NMR spectroscopic broadening in only these two sets of protons is strongly supportive of the predicted structure.

The ^{13}C NMR spectrum of **9** was found to support the formula of $(Tp^H)(Bp^{Ph})YBr$, but was not informative as to its geometry. Without a mirror plane of symmetry, $(Tp^H)(Bp^{Ph})YBr$ (**9**) would be expected to give rise to 10 separate carbon resonances, these having being observed and identified in the ^{13}C NMR spectrum. The C-4 carbon atoms of both ligands appear as singlets at 104.88 and 104.60 ppm. The intensities of these peaks appear correctly in the expected 3:2 ratio and can be assigned to the Tp^H C-4 and the Bp^{Ph} C-4, respectively. The four unique carbon positions belonging to the two equivalent phenyl substituents are observed in the expected aromatic region of the spectrum. The remaining four types of carbon nuclei belonging to the different pyrazolyl groups appear as two sets of peaks in the expected regions of the spectrum: the C-5 carbons of the Tp^H and Bp^{Ph} ligands are visible at 136.74 and 132.41 ppm, respectively, while the C-3 carbons appear at 144.50 and 154.63 ppm. Interestingly, the peak observed at 154.63 ppm, corresponding to the C-3 carbons of the Bp^{Ph} ligand, appears either as two closely spaced singlets or as a true doublet with a small coupling to the NMR-active yttrium nuclei equal to $J = 1.46$ Hz.

Although ^{1}H NMR spectroscopy strongly supports the predicted octahedral structure of $(Tp^H)(Bp^{Ph})YBr$ (**9**), it does not offer any evidence as to why the expected effects of a mirror plane in the complex are not observed. As previously mentioned, the steric interactions between the phenyl groups and the Tp^H ligand may be causing fluxional behavior in solution which could equilibrate the pyrazolyl signals from the Tp^H ligand. This fluxional behavior may take the form of an on/off dissociation equilibrium for the Bp^{Ph} pyrazolyl nitrogens, which are forced off the yttrium center due to steric interactions with its phenyl substituents, or to an equilibration of the yttrium coordination sphere caused by a solvent interaction, as seen with the previous $Tp^RYX_2(THF)$ complexes. Some supporting evidence for the latter theory was found by again changing the deuterated solvent for the complex during NMR spectroscopic analysis. It would be expected, as we had previously seen, that the fluxional behavior of **9** could be influenced by coordinating and noncoordinating solvents. As already illustrated, the ^{1}H NMR spectrum of **9** taken in $CDCl_3$ shows a single H-4 triplet for the Tp^H ligand at 6.07 ppm. However, when taken in d_6-benzene, the proton spectrum shows an additional triplet at 5.96 ppm, and the resonances of the Tp^H H-3 and the ortho-phenyl protons shift downfield by 0.2 to 0.55 ppm. Although the additional triplet does not properly integrate to a ratio of 2:1 with its much larger neighboring triplet at 6.07 ppm, its appearance in the noncoordinating benzene solvent supports the idea that, as solvent interaction with the complex decreases, structures characterized by inequivalent Tp^H pyrazolyl groups will have an increasingly long lifetime and will be increasingly able to be observed on the NMR time scale.

Conclusions. The syntheses of a series of well-characterized complexes of the type Tp^RYX_2(solvent) are presented. The data demontrates that the steric, dynamic, and coordination behavior of these complexes is heavily influenced by the choice of Tp ligand substituents, showing the versatility of this ligand system for catalyst design. Also, the lack of ligand redistribution seen again is favorable for complexes of these ligands as catalyst precursors. The derivatization of these complexes by alkyls gives highly active olefin polymerization catalysts, the properties of which differ from their metallocene analogues.[19] Further manipulation of ligand steric demands is being explored to accommodate various lanthanide metals and to control or direct their catalytic activity.

Syntheses of the new bispoly(pyrazolyl)borohydride yttrium monohalide complexes which are devoid of coordinating solvents, $[(Tp^R)(Bp^{R'})YX]$, have also been presented. These unsolvated monohalide yttrium complexes should prove to be excellent precursors to monoalkyl or hydride derivatives. Research into the potential catalytic olefin polymerization activity of complexes of the type $(Tp^H)(Bp^{R'})YR$ (R = H, alkyl) is currently underway.

Experimental Section

General. All reactions and procedures were carried out in an inert atmosphere of argon using standard glovebox and Schlenk techniques. Toluene, THF, and pentane (Baker-analyzed, VWR) were distilled from sodium/benzophenone ketyl under an inert atmosphere. Methylene chloride, chloroform, and chlorobenzene were dried over and distilled from calcium hydride. NaTp was obtained from Aldrich, and anhydrous YCl_3 and YBr_3 were obtained from Strem Chemicals, and were all used as received. KTp^{Me}, KTp^{Ph}, KBp^{Me}, KBp^{Ph}, and $NdI_3(THF)_4$ were synthesized using literature procedures.[23,24] NMR spectroscopy was carried out on Bruker instruments operating at 200 MHz for ^{1}H and 75 MHz for ^{13}C. Molecular mechanics (MM2) calculations were used to

(23) (a) Trofimenko, S. *J. Am. Chem. Soc.* **1967**, *89*, 6288. (b) Trofimenko, S.; Calabrese, J. C.; Thompson, J. S. *Inorg. Chem.* **1987**, *26*, 1507.
(24) Hazin, P. N.; Huffman, J. C.; Bruno, J. W. *Organometallics* **1987**, *6*, 23.

Table 4. Crystallographic Data for $Tp^{Me}YCl_2$(3,5-dimethylpyrazole)·$^1/_2CH_2Cl_2$ (**5**·$^1/_2CH_2Cl_2$), $Tp^HNdI_2(THF)_2$ (**3**), and $Tp^{Me}NdI_2(THF)$·CH_2Cl_2 (**6**·CH_2Cl_2)

	5·$^1/_2CH_2Cl_2$	**3**	**6**·CH_2Cl_2
formula	$C_{20}H_{30}N_8Cl_2BY$·$0.5CH_2Cl_2$	$C_{17}H_{26}BI_2N_6NdO_2$	$C_{20}H_{32}BCl_2I_2N_6NdO$
fw	595.60	755.05	852.3
space group	$C2/c$ (C_{2h}^6; No. 15)	$P\bar{1}$ (C_i^1; No. 2)	$P2_1/c$ (C_{2h}^5; No. 14)
a (Å)	20.800(7)	10.0562(14)	10.847(4)
b (Å)	10.990(3)	12.4746(16)	15.820(5)
c (Å)	25.177(4)	12.5080(18)	18.312(5)
α (deg)		92.412(11)	
β (deg)	96.04(2)	91.697(12)	101.13(3)
γ (deg)		113.358(10)	
V (Å^3)	5723(3)	1437.4(5)	3083.2(11)
Z	8	2	4
D_{calcd} (g/cm^3)	1.382	1.746	1.836
μ(Mo Kα) (mm^{-1})	2.342	3.98	3.88
temp, °C	23 ± 2	25 ± 2	22 ± 2
λ(Mo Kα) (Å)	0.71073	0.71073	0.71073
R^a	0.0525	0.0793	0.0744
R_w	0.1092[b]	0.0929[c]	0.0977[c]

[a] $R(F) = \Sigma||F_o| - |F_c||/\Sigma|F_o|$. [b] $R_w(F_o^2) = \{\Sigma w(F_o^2 - F_c^2)^2/\Sigma wF_o^4\}$. [c] $R(wF) = \Sigma\,[|F_o| - |F_c|]w^{0.5}/\Sigma|F_o|w^{0.5}$.

arrive at energy-minimized conformations and geometries in order to generate space-filling models of **8** and **9** (see Supporting Information). In these calculations the atoms of the yttrium coordination sphere were held in fixed coordinates derived from the crystal structure of **5**, while the remaining atoms were allowed to minimize conformation and geometry. Chemical analyses were obtained by the Microanalytical Laboratory of the Materials Research Science and Engineering Center at the University of Massachusetts at Amherst.

[Tp^{H}YX$_2$(THF)$_2$] [X = Br (1) and Cl (2)]. Anhydrous YBr_3 (3.00 g, 9.13 mmol) or anhydrous YCl_3 (3.31 g, 9.13 mmol) was stirred with 100 mL of anhydrous THF. At room temperature the metal halides only partially dissolve. To the stirring mixture was added $NaTp^H$ (2.15 g, 9.13 mmol) as a powder slowly over 15 min. After the complete addition, the mixture was stirred at room temperature for 2 days. The stirring was then stopped to allow the alkali metal halide precipitate to settle out of the reaction, which occurred after 2 days. The mixture was carefully decanted through a fine filter to fully separate the NaBr or NaCl from the solution. After filtration, the clear and colorless filtrate was reduced in volume under vacuum until the solution was saturated. Pentane was slowly added dropwise to precipitate the product, which was collected by filtration and dried. This initial product was then extracted into a mixture of toluene and THF (5:1 v/v) with stirring. The resulting cloudy mixture was again filtered to remove the remaining insoluble material, and the filtrate was again reduced in volume until saturated. Slow addition of pentane resulted in the precipitation of a crystalline white powder, which was collected and dried under vacuum for several days. The final product was isolated as a microcrystalline white powder, yield 91% (5.04 g) for **1** and 89% for **2**.

[Tp^{H}YBr$_2$(THF)$_2$] (1). Anal. Calcd for $C_{17}H_{26}N_6O_2BBr_2Y$: C, 33.7; H, 4.3; N, 13.9; Br, 26.4. Found: C, 33.8; H, 4.24; N, 13.74; Br, 27.5. ^{1}H NMR ($CDCl_3$): δ = 1.92 (mult, 10.2 H, THF), 3.99 (mult, 10.1 H, THF), 6.16 (t, 3.00 H, H-4, J_{H-H} = 2.16 Hz), 7.65 (d, 3.10 H, H-3, J_{H-H} = 1.80 Hz), 8.05 (d, 2.97 H, H-5, J_{H-H} = 1.80 Hz). ^{13}C{^{1}H} NMR ($CDCl_3$): δ = 25.7 (s, THF), 71.1 (s, THF), 105.0 (s, C-4), 136.4 (s, C-3), 143.7 (s, C-5).

[Tp^{H}YCl$_2$(THF)$_2$] (2). ^{1}H NMR (d_8-THF): δ = 6.10 (t, H-4, J_{H-H} = 2.12 Hz), 7.67 (d, H-3, J_{H-H} = 2.15 Hz), 7.98 (d, H-5, J_{H-H} = 1.97 Hz), 4.58 (q, B−H, J_{B-H} = 130.1 Hz).

[Tp^{H}NdI$_2$(THF)$_2$] (3). This procedure is a modification of that described in ref 15. $NdI_3(THF)_4$ (6.47 g, 7.95 mmol) and KTp^H (2.01 g, 7.95 mmol) were added to a flask with 60 mL of anhydrous THF. This mixture was stirred for 24 h at room temperature. During this time, the solution became blue, and white KI precipitated. The solution was filtered to remove KI and rotovaped to a dry blue powder. This powder was dissolved in 30 mL of CH_2Cl_2, filtered, and reduced in volume until saturated. Pentane was slowly added until the product precipitated. The blue solid was collected by filtration, washed with pentane, and dried under vacuum. The yield of **3** was 4.5 g, 75%. Anal. Calcd for $C_{17}H_{26}N_6O_2BI_2Nd$: C, 27.0; H, 3.47; N, 11.13; I, 33.60; Nd, 19.10. Found: C, 26.93; H, 3.47; N, 14.38; I, 35.22; Nd, 17.97. ^{1}H NMR (CD_2Cl_2): δ = 0.90 (br, H-3), 5.70 (br, THF), 7.67 (s, H-5), 8.49 (br, THF), 11.94 (br, H-4).

[Tp^{Me}YCl$_2$(THF)] (4). In a typical experiment, 6.00 g (17.84 mmol) of potassium hydrotris(3,5-dimethylpyrazolyl)borate (KTp^{Me}) and 3.47 g (17.84 mmol) of YCl_3 were added to a flask with 200 mL of anhydrous THF. This milky-colored mixture was stirred at room temperature for 3 days, during which the amount of insoluble material dramatically decreased and the color of the mixture changed to faded white with a slight bluish tint, indicative of a fine ionic salt. The stirring was then stopped and the reaction mixture was left undisturbed, permitting the separation of the fine salt from the solution. Once the salt had adequately settled, the mixture was decanted through a fine filter. The clear and colorless filtrate was reduced in volume until saturated. Slow addition of pentane precipitated a white powder, which was collected, dried, and then extracted into a mixture of toluene and THF (5:1 v/v). The resulting murky solution was again filtered to remove the remaining insoluble materials, and the clear filtrate was again reduced in volume until saturated, with pentane then slowly added to precipitate the product. Additional extraction and recrystallization steps can be performed using CH_2Cl_2/pentane to further purify the product. $Tp^{Me}YCl_2(THF)$ (**4**) was isolated as a fine white powder in about 90% yield. Anal. Calcd for $C_{19}H_{30}N_6OBCl_2Y$: C, 43.13; H, 5.71; N, 15.88; Cl, 13.40. Found: C, 42.82; H, 5.36; N, 15.88; Cl, 13.60. ^{1}H NMR (d_6-benzene): δ = 1.16 (mult, 4 H, THF), 2.09 (s, 9 H, 5-Me), 2.57 (br s, 7 H, 3-Me), 3.74 (mult, 4 H, THF), 5.42 (s, 3 H, H-4). ^{13}C{^{1}H} NMR (d_8-THF): 12.86 (s, 5-Me), 14.14 (s, 3-Me), 106.5 (s, C-4), 146.2 (s, C-3), 151.3 (s, C-5).

[Tp^{Me}NdI$_2$(THF)] (6). This procedure is a modification of that described in ref 15. $NdI_3(THF)_4$ (3.39 g, 4.17 mmol) and KTp^{Me} (1.37 g, 4.66 mmol) were added to a flask with 60 mL of anhydrous THF. This mixture was stirred for 24 h at room temperature. During this time, the solution became blue, and white KI precipitated. The solution was filtered to remove KI and rotovaped to a dry blue powder. This powder was dissolved in 30 mL of CH_2Cl_2, filtered, and reduced in volume until saturated. Pentane was slowly added until the product precipitated. The blue solid was collected by filtration, washed with pentane, and dried under vacuum. The yield of **6** was 2.36 g, 78%. Anal. Calcd for $C_{19}H_{30}N_6OBI_2Nd$: C, 29.9; H, 3.94; N, 10.95; I, 33.08; Nd, 18.79. Found: C, 28.99; H, 3.93; N, 10.22; I, 35.67; Nd, 17.61. ^{1}H NMR ($CDCl_3$): δ = −5.81 (br, 3-Me), 2.28 (br, THF), 3.94 (br, THF), 4.75 (s, 9 H, 5-Me,), 8.24 (s, 3 H, H-4).

[Tp^{Ph}YCl$_2$(THF)] (7). In a typical procedure anhydrous YCl_3 (2.00 g, 10.24 mmol) and potassium hydrotris(3-phenylpyrazolyl)borate (KTp^{Ph}) (4.92 g, 10.24 mmol) were added to a flask with 200 mL of anhydrous THF. This mixture was stirred for 3 days at room temperature. The stirring was then stopped to permit the insoluble KCl to settle to the bottom of the vessel. The clear solution was decanted through a fine filter, and the solvent was removed under vacuum. The

Table 5. Selected Bond Distances (Å) and Angles (deg) for $Tp^{H}NdI_2(THF)_2$ (**3**) and $Tp^{Me}NdI_2(THF)\cdot CH_2Cl_2$ (**6**·CH_2Cl_2)[a]

3		**6**·CH_2Cl_2	
Nd−N(1)	2.517(16)	Nd−N(1)	2.461(13)
Nd−N(3)	2.503(19)	Nd−N(3)	2.499(13)
Nd−N(5)	2.495(24)	Nd−N(5)	2.521(15)
Nd−O(1)	2.458(17)	Nd−O(1)	2.415(14)
Nd−O(2)	2.500(16)		
Nd−I(1)	3.062(3)	Nd−I(1)	3.040(2)
Nd−I(2)	3.136(3)	Nd−I(2)	3.055(2)
N(1)−Nd−N(3)	74.6(6)	N(1)−Nd−N(3)	79.5(4)
N(1)−Nd−N(5)	70.6(7)	N(1)−Nd−N(5)	77.0(5)
N(3)−Nd−N(5)	75.8(7)	N(3)−Nd−N(5)	75.2(5)
N(1)−Nd−O(1)	70.5(6)	O(1)−Nd−N(1)	159.5(5)
N(1)−Nd−O(2)	142.0(7)		
N(3)−Nd−O(1)	98.5(6)	O(1)−Nd−N(3)	85.1(4)
N(3)−Nd−O(2)	95.4(6)		
N(5)−Nd−O(1)	140.7(6)	O(1)−Nd−N(5)	86.1(5)
N(5)−Nd−O(2)	71.4(6)		
O(1)−Nd−O(2)	147.4(5)		
I(1)−Nd−N(1)	96.7(5)	I(1)−Nd−N(1)	94.4(3)
I(1)−Nd−N(3)	167.1(5)	I(1)−Nd−N(3)	92.3(4)
I(1)−Nd−N(5)	92.4(5)	I(1)−Nd−N(5)	165.8(3)
I(2)−Nd−N(1)	137.7(5)	I(2)−Nd−N(1)	102.0(3)
I(2)−Nd−N(3)	87.1(5)	I(2)−Nd−N(3)	171.3(4)
I(2)−Nd−N(5)	141.4(5)	I(2)−Nd−N(5)	96.7(3)
I(1)−Nd−O(1)	87.3(4)	I(1)−Nd−O(1)	99.7(4)
I(1)−Nd−O(2)	85.6(4)		
I(2)−Nd−O(1)	75.1(4)	I(2)−Nd−O(1)	91.2(3)
I(2)−Nd−O(2)	76.3(4)		
I(1)−Nd−I(2)	105.7(1)	I(1)−Nd−I(2)	96.1(1)

[a] Atoms are labeled to agree with Figure 2 and Figure 6. Esd's in parentheses.

resulting glassy material was extracted into toluene which had a small amount of THF included, filtered, and reduced in volume until saturated, and then pentane was slowly added until the product precipitated. This procedure was repeated, and the resulting white powder was dried for several days under vacuum. The yield of the reaction can exceed 70% depending on the number of extractions performed. Anal. Calcd for $C_{31}H_{30}N_6OBCl_2Y$: C, 55.31; H, 4.49; N, 12.48; Cl, 10.53. Found: C, 56.27; H, 4.40; N, 13.18; Cl, 10.51. ^{1}H NMR (d_8-THF): δ = 1.73 (mult, THF), 3.58 (mult, THF), 6.26−8.45 (br mult, Tp^{Ph} protons).

[(Tp^{Me})(Bp^{Me})YCl] (8). Analytically pure $Tp^{Me}YCl_2(THF)$ (**4**, 0.459 g, 0.867 mmol) was dissolved in 30 mL of THF, and the clear, colorless solution was then diluted to 100 mL by the addition of toluene. With stirring, 1 equiv of KBp^{Me} (0.21 g, 0.867 mmol) was added to the solution in very small aliquots over 20 min as a powder. As the addition proceeded, the solution slowly became cloudy as insoluble KCl began to precipitate. After the addition was complete, the reaction mixture was stirred overnight at room temperature and then warmed to approximately 60 °C with stirring for an additional day to ensure the complete reaction of the KBp^{Me}. On the following day the mixture was filtered to remove the insoluble KCl, giving a clear colorless filtrate, which was reduced in volume under vacuum until the solution was composed mainly of toluene and was saturated with the product. Pentane was added slowly, precipitating a white powder. This powder was collected and then redissolved in CH_2Cl_2, filtered, and recrystallized by the addition of excess pentane. The purified product was then dried under vacuum. The final product was a fine white powder, 0.38 g, approximately 70% yield. Anal. Calcd for $C_{25}H_{38}N_{10}ClB_2Y$: C, 48.9; H, 6.2; N, 22.8; Cl, 5.8. Found: C, 47.41; H, 5.94; N, 22.08; Cl, 6.2. ^{1}H NMR ($CDCl_3$): δ = 0.534 (s, 3 H, Tp^{Me} 3-Me), 1.39 (s, 6 H, 2 Bp^{Me} 3-Me), 2.38 (br s, overlapping peaks, 9 H, Tp^{Me} 5-Me and 2 Tp^{Me} 3-Me), 2.43 and 2.44 (2 peaks, 12 H, 2 Tp^{Me} 5-Me and 2 Bp^{Me} 5-Me), 5.52 (s, 1 H, Tp^{Me} H-4), 5.67 (s, 2 H, 2 Tp^{Me} H-4), 5.77 (s, 2 H, 2 Bp^{Me} H-4). ^{13}C{^{1}H} NMR ($CDCl_3$): δ = 9.66 (s, 1 Tp^{Me} 3-Me), 11.67 (s, 2 Bp^{Me} 3-Me), 11.92 (s, 2 Tp^{Me} 3-Me), 13.02 (s, 2 Bp^{Me} 5-Me), 13.17 (s, 1 Tp^{Me} 5-Me), 14.39 (s, 2 Tp^{Me} 5-Me), 105.63 (s, 2 Bp^{Me} C-4), 105.78 (s, 3 Tp^{Me} C-4), 144.32 (s, 1 Tp^{Me} C-3), 145.02 and 145.15 (s, 2 Tp^{Me} C-3 and Bp^{Me} C-3), 149.4 and 150.69 (s, 2 Tp^{Me} C-5 and 2 Bp^{Me} C-5), 150.77 (s, 1 Tp^{Me} C-5).

[(Tp^{H})(Bp^{Ph})YBr] (9). Analytically pure $Tp^{H}YBr_2(THF)_2$ (**1**, 2.00 g, 3.3 mmol) was mixed with 100 mL of anhydrous toluene, in which the complex did not fully dissolve. $TlBp^{Ph}$ (1.66 g, 3.3 mmol) was slowly added to this stirring mixture as a dry powder in small increments over about 30 min. During the addition of the $TlBp^{Ph}$ the appearance of the mixture changed, taking on a slight orange color as insoluble thallium bromide began to precipitate from the toluene solution. After the complete addition of $TlBp^{Ph}$, the reaction mixture was stirred at room temperature overnight. Stirring was then stopped to allow the TlBr to settle to the bottom of the flask, and the toluene solution was decanted through a fine filter, yielding a clear, colorless filtrate containing the product. The toluene was reduced in volume until the solution was saturated, and pentane was slowly added dropwise (about 150 mL total), causing a white powder to precipitate. This crude product was collected and extracted into a mixture of toluene and CH_2Cl_2 (10:1), filtered, and recrystallized by addition of pentane at −20 °C. This extraction and recrystallization was repeated three more times. The purified product was then collected and dried under vacuum, giving 1.85 g (82.3% yield) of [(Tp^{H})(Bp^{Ph})YBr] (**9**) as a fluffy white powder. Anal. Calcd for $C_{27}H_{26}N_{10}BrB_2Y$: C, 47.62; H, 3.85; N, 20.57; Br, 11.73. Found: C, 48.58; H, 3.93; N, 19.78; Br, 13.7. ^{1}H NMR ($CDCl_3$): δ = 6.07 (t, 3 H, J_{H-H} = 2.18 Hz, Tp^{H} H-4), 6.45 (d, 2 H, J_{H-H} = 2.18 Hz, Bp^{Ph} H-4), 7.14 (br mult, overlapping peaks, 6 H, para and meta Ph-H), 7.4 (br mult, 4 H, ortho Ph-H), 7.50 (br d, 3 H, Tp^{H} H-3), 7.57 (d, 2 H, J_{H-H} = 2.18 Hz, Bp^{Ph} H-5), 7.68 (d, 3 H, J_{H-H} = 1.70 Hz, Tp^{H} H-5). ^{13}C{^{1}H} NMR ($CDCl_3$): δ = 104.6 (s, 2 Bp^{Ph} C-4), 104.9 (s, 3 Tp^{H} C-4), 127.3 and 128.5 (s, 4 ortho and 4 meta Ph-C), 128.5 (s, 2 para Ph-C), 132.4 (s, 2 Bp^{Ph} C-5), 136.7 (s, 3 Tp^{H} C-5), 137.2 (s, 2 ipso Ph-C), 144.5 (s, 3 Tp^{H} C-3), 154.6 (d, J = 1.46 Hz, 2 Bp^{Ph} C-3).

X-ray study of $Tp^{Me}YCl_2$(3,5-dimethylpyrazole)·$^1/_2CH_2Cl_2$ (5·$^1/_2CH_2Cl_2$). The X-ray crystallographic study was carried out using an Enraf-Nonius CAD4 diffractometer and graphite-monochromated Mo Kα radiation (λ = 0.71073 Å). Details of the experimental procedures have been described previously.[25]

The colorless crystal was mounted under an argon atmosphere in a thin-walled glass capillary tube, which was then sealed. Data were collected using the $\Theta-2\Theta$ scan mode with $2° \le 2\Theta_{MoK\alpha} \le 50°$ at 23 ± 2 °C. A total of 5014 independent reflections ($+h$, $+k$, $\pm l$) was measured. An empirical absorption correction based on ψ scans was applied (relative transmission factors from 0.739 to 1.00 on I). The structure was solved by direct methods and difference Fourier techniques and was refined by full-matrix least-squares. During solution of the structure a methylene chloride of solvation was located with its carbon atom lying on a crystallographic 2-fold axis. Since the atoms of the complex are in general positions, there is a half molecule of methylene chloride per molecule of complex.

All of the data were included in the refinement, which was based on F^2. Computations were performed on a Pentium Pro 200 computer using SHELXS-86 for solution[26] and SHELXL-93 for refinement.[27] Non-hydrogen atoms were refined anisotropically. Hydrogen atoms were included in the refinement as isotropic scatterers riding either in ideal positions or with torsional refinement (in the case of methyl hydrogen atoms) on the bonded carbon atoms. The final agreement factors are based on the 2447 reflections with $I \ge 2\sigma_I$. Crystallographic data are summarized in Table 4.

X-ray studies of $Tp^{H}NdI_2(THF)_2$ (3) and $Tp^{Me}NdI_2(THF)\cdot CH_2Cl_2$ (6) A Siemens P4 diffractometer was used to collect data at ambient conditions. The pale blue crystals were mounted in sealed thin-wall capillary tubes under an argon atmosphere. A total of 4854 reflections (3177 independent) were measured for **3**, and a total of 5218 reflections (4840 independent) were measured for **6**. No symmetry higher than triclinic was observed for **3**, and the centrosymmetric option was chosen

(25) Sau, A. C.; Day, R. O.; Holmes, R. R. *Inorg. Chem.* **1981**, *20*, 3076.
(26) Sheldrick, G. M. *Acta Crystallogr.* **1990**, *A46*, 467.
(27) (a) Sheldrick, G. M. *SHELXL-93: program for crystal structure refinement*; University of Göttingen: Göttingen, 1993. (b) ORTEX 5e, McArdle, P. Crystallography Centre, Chemistry Department, University College, Galway, Ireland.

on the basis of the stability of the refinement process. The structures were solved by direct methods and completed by subsequent difference Fourier syntheses. Complex **6** was found to contain a molecule of CH_2Cl_2 for each Nd complex. Complex **3** contained a disordered, probably substoichiometric, chemically unidentified small molecule represented by three carbon atoms (C21−C23). The formula, formula weight, and density in Table 4 do not include these atoms. A full disclosure is available in the Supporting Information. Full-matrix least-squares refinement used anisotropic thermal parameters for all non-hydrogen atoms for **6**. Hydrogen atoms were treated as idealized contributions. All software was contained in the SHELXTL library version 4.05.[27] Selected bond lengths and angles are shown in Table 5, and crystallographic data are summarized in Table 4.

Acknowledgment. We thank Dr. Charles Dickinson and Li Qiang of the University of Massachusetts at Amherst for acquisition of NOE data. We also thank the University of Massachusetts for support of this work.

Supporting Information Available: Space-filling models of **8** and **9** generated by molecular mechanics (MM2) calculations, tables of crystal and refinement data, atomic coordinates, bond lengths and angles, anisotropic thermal parameters, and fixed hydrogen atom parameters for **3**, **5**·0.5 CH_2Cl_2, and **6**·CH_2Cl_2. This material is available free of charge via the Internet at http://pubs.acs.org.

IC991179L